Article

Ab Initio QM/MM Study of Class A β-Lactamase Acylation: Dual Participation of Glu166 and Lys73 in a Concerted Base Promotion of Ser70

Samy O. Meroueh, Jed F. Fisher, H. Bernhard Schlegel, and Shahriar Mobashery

J. Am. Chem. Soc., **2005**, 127 (44), 15397-15407• DOI: 10.1021/ja051592u • Publication Date (Web): 14 October 2005

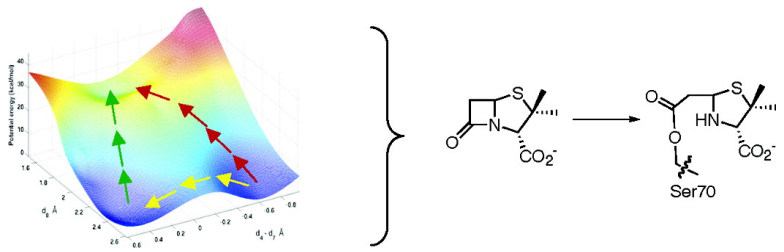

More About This Article

Additional resources and features associated with this article are available within the HTML version:

- Supporting Information
- Links to the 10 articles that cite this article, as of the time of this article download
- Access to high resolution figures
- Links to articles and content related to this article
- Copyright permission to reproduce figures and/or text from this article

View the Full Text HTML

J|A|C|S
ARTICLES
Published on Web 10/14/2005

Ab Initio QM/MM Study of Class A β-Lactamase Acylation: Dual Participation of Glu166 and Lys73 in a Concerted Base Promotion of Ser70

Samy O. Meroueh,[†] Jed F. Fisher,[†] H. Bernhard Schlegel,[‡] and Shahriar Mobashery*,[†]

Contribution from the Department of Chemistry and Biochemistry, University of Notre Dame, Notre Dame, Indiana 46556, and Department of Chemistry, Wayne State University, Detroit, Michigan 48202

Received March 12, 2005; E-mail: mobashery@nd.edu

Abstract: β-Lactamase acquisition is the most prevalent basis for Gram-negative bacteria resistance to the β-lactam antibiotics. The mechanism used by the most common class A Gram-negative β-lactamases is serine acylation followed by hydrolytic deacylation, destroying the β-lactam. The ab initio quantum mechanical/molecular mechanical (QM/MM) calculations, augmented by extensive molecular dynamics simulations reported herein, describe the serine acylation mechanism for the class A TEM-1 β-lactamase with penicillanic acid as substrate. Potential energy surfaces (based on approximately 350 MP2/6-31+G* calculations) reveal the proton movements that govern Ser70 tetrahedral formation and then collapse to the acyl-enzyme. A remarkable duality of mechanism for tetrahedral formation is implicated. Following substrate binding, the pathway initiates by a low energy barrier (5 kcal mol^{-1}) and an energetically favorable transfer of a proton from Lys73 to Glu166, through the catalytic water molecule and Ser70. This gives unprotonated Lys73 and protonated Glu166. Tetrahedral formation ensues in a concerted general base process, with Lys73 promoting Ser70 addition to the β-lactam carbonyl. Moreover, the three-dimensional potential energy surface also shows that the previously proposed pathway, involving Glu166 as the general base promoting Ser70 through a conserved water molecule, exists in competition with the Lys73 process. The existence of two routes to the tetrahedral species is fully consistent with experimental data for mutant variants of the TEM β-lactamase.

Introduction

β-Lactam antibiotics acylate an active site serine of penicillin-binding proteins (PBPs), a reaction that deprives bacteria of the PBP enzymatic activity and kills the microorganism. It is widely accepted that β-lactamases, resistance enzymes to β-lactam antibiotics, have evolved from PBPs by acquiring the ability to hydrolyze rapidly the acyl-enzyme species.[1−4] These evolutionary steps have given rise to four distinct β-lactamase types (classes A−D).[3,5] Despite numerous X-ray crystallographic structures (including two ultrahigh-resolution structures),[6,7] the class A β-lactamase acylation mechanism is still debated, largely due to the complex ensemble of amino acid residues proximal to the bound β-lactam substrate. In addition to the nucleophilic serine (Ser70) this ensemble includes Lys73, Glu166, Ser130, and Lys234 (Figure 1A).

It is widely accepted that the evolutionary introduction of Glu166 to the active site of the class A β-lactamases enables the promotion of the water molecule for catalytic acyl-enzyme hydrolysis.[1,8] As the lysine located three residues to the *C*-terminal side of the nucleophilic serine in PBPs is required for serine acyl-enzyme formation in these enzymes, the retention of this lysine in the β-lactamases implies a critical contribution to the β-lactamase acylation mechanism as well. The precise role of this lysine is, however, uncertain. In the class A β-lactamases the pK_a of this lysine *in the free enzyme* is 8.0−8.5.[9] The suppression of the Lys73 pK_a is a consequence of three particular features of the active site: the hydrophobicity of the amino acids (apart from Ser70, Asp166, and Lys234) that surround the Lys73 amine, the nearly complete solvent shielding of this lysine (as distinct from the solvent exposed Lys234 amine), and most importantly the proximity of the Lys234 (a lysine with a normal pK_a).[9] The close interrelatedness of Lys73 with the other active site amino acids is emphasized

[†] University of Notre Dame.
[‡] Wayne State University.

(1) Knox, J. R.; Moews, P. C.; Frere, J. M. *Chem. Biol.* **1996**, *3*, 937−47.
(2) Frere, J. M.; Dubus, A.; Galleni, M.; Matagne, A.; Amicosante, G. *Biochem. Soc. Trans.* **1999**, *27*, 58−63.
(3) Fisher, J. F.; Meroueh, S. O.; Mobashery, S. *Chem. Rev.* **2005**, *105*, 395−424.
(4) Labia, R. *Curr. Med. Chem.: Anti-Infect. Agents* **2004**, *3*, 251−266.
(5) Bush, K.; Jacoby, G. A.; Medeiros, A. A. *Antimicrob. Agents Chemother.* **1995**, *39*, 1211−1233.
(6) Nukaga, M.; Mayama, K.; Hujer, A. M.; Bonomo, R. A.; Knox, J. R. *J. Mol. Biol.* **2003**, *328*, 289−301.
(7) Minasov, G.; Wang, X.; Shoichet, B. K. *J. Am. Chem. Soc.* **2002**, *124*, 5333−40.
(8) Massova, I.; Mobashery, S. *Antimicrob. Agents Chemother.* **1998**, *42*, 1−17.
(9) Golemi-Kotra, D.; Meroueh, S. O.; Kim, C.; Vakulenko, S. B.; Bulychev, A.; Stemmler, A. J.; Stemmler, T. L.; Mobashery, S. *J. Biol. Chem.* **2004**, *279*, 34665−34673.

10.1021/ja051592u CCC: $30.25

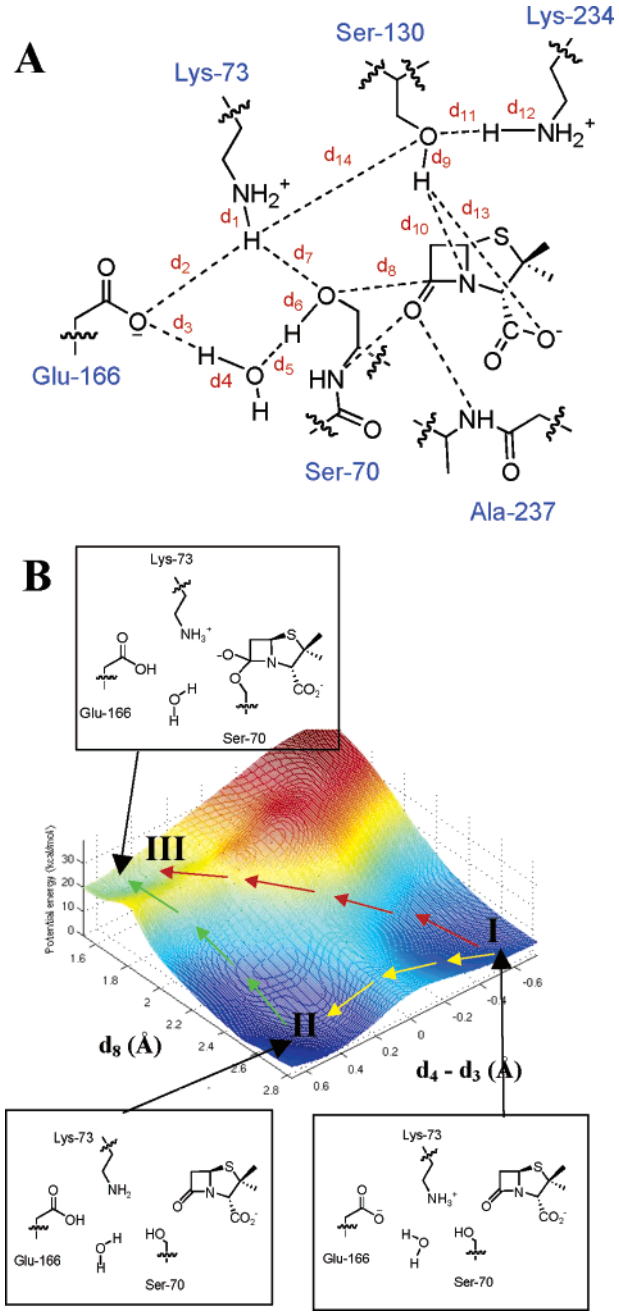

Figure 1. (A) Schematic representing the residues that were included in the QM region during the ONIOM QM/MM calculations. (B) Potential energy surface for the formation of the tetrahedral intermediate. All points used to construct the surface were determined at the MP2/6-31+G* level. A schematic of the species representing each stable species on the potential energy surface is also shown, with arrows pointing to their respective minimum on the surface.

by an even greater change in the Glu166Ala mutant (pK_a = 6.0). This change reflects the electrostatic effect of Glu166, which is only 2.8−3.4 Å distant.[9,10] While Lys73 is protonated upon encounter with the substrate (free enzyme pK_a = 8.0−8.5), the possibility that Lys73 acts as a base in catalysis cannot be excluded. Nonetheless, the fact that Lys73 is protonated in the initial Michaelis complex has been argued as favoring Glu166 as the catalytic base in acylation, in addition to its role in deacylation.[11] Yet mutation of Glu166 (to Gln) decreases by as much as 100−1000-fold but does not abolish the microscopic rate constant for acylation (an attenuation of 6 orders of magnitude of the microscopic rate constant for deacylation is also seen).[11,12] Indeed, X-ray structures of acyl-enzymes for the TEM-1 Glu166Asn mutant[13] and the *Bacillus licheniformis* 749/C Glu166Ala mutant[14] β-lactamases exist, indicating that acylation is possible in the absence of the Glu166 carboxylate but deacylation is not. *This presents a paradox for Ser70 activation: Lys73 is protonated and Glu166 appears not essential*.

Resolution of such paradoxes is possible by computational study, and for this reason the class A acylation pathway has received vigorous scrutiny. These studies include force-field-based methods,[9,15−19] model system quantum mechanical study,[16,20] and semiempirical QM/MM study.[21−24] We present here the first ab initio molecular orbital QM/MM study (using explicit solvation) of the two-step process of serine acyl-enzyme formation: serine addition to the β-lactam carbonyl to form a tetrahedral species and the tetrahedral collapse to the acyl-enzyme. Our calculations use two-layer ONIOM methodology with electrostatic embedding[25] as implemented in the Gaussian03 programs. These calculations are complemented with extensive molecular dynamics simulations with explicit solvent and provide new insight into the acylation reaction mechanism.

Computational Methods

The TEM-1 β-lactamase X-ray structure (PDB code 1BTL) provided the Cartesian coordinates for the molecular dynamics simulations and QM/MM calculations. The Michaelis complex of TEM-1 with penicillanic acid was constructed as described.[26] The enzyme was protonated using the Protonate program of AMBER 7 to assign standard protonation states to ionizable residues.[27] Protonation of penicillanic acid was carried out using Sybyl 6.91 (Tripos Inc., St. Louis, MO), and atomic charges for penicillanic acid in the Michaelis complex and in the tetrahedral species were determined using RESP methodology, using a HF/6-31+G(d) single-point energy calculation to determine the electrostatic potential around the molecule for a two-stage RESP fitting procedure.[28] Force field parameters for the protein were assigned from the "parm99" set of parameters, while the substrate parameters were obtained from the "gaff" parameters within AMBER 7. The complex

(10) Ibuka, A. S.; Ishii, Y.; Galleni, M.; Ishiguro, M.; Yamaguchi, K.; Frere, J. M.; Matsuzawa, H.; Sakai, H. *Biochemistry* **2003**, *42*, 10634−43.
(11) Guillaume, G.; Vanhove, M.; Lamotte-Brasseur, J.; Ledent, P.; Jamin, M.; Joris, B.; Frere, J. M. *J. Biol. Chem.* **1997**, *272*, 5438−5444.
(12) Gibson, R. M.; Christensen, H.; Waley, S. G. *Biochem. J.* **1990**, *272*, 613−9.
(13) Strynadka, N. C.; Adachi, H.; Jensen, S. E.; Johns, K.; Sielecki, A.; Betzel, C.; Sutoh, K.; James, M. N. *Nature* **1992**, *359*, 700−5.
(14) Knox, J. R.; Moews, P. C.; Escobar, W. A.; Fink, a. L. *Protein Eng.* **1993**, *6*, 11−18.
(15) Diaz, N.; Sordo, T. L.; Merz, K. M.; Suarez, D. *J. Am. Chem. Soc.* **2003**, *125*, 672−684.
(16) Massova, I.; Kollman, P. A. *J. Comput. Chem.* **2002**, *23*, 1559−76.
(17) Atanasov, B. P.; Mustafi, D.; Makinen, M. W. *Proc. Natl. Acad. Sci. U.S.A.* **2000**, *97*, 3160−5.
(18) Oliva, M.; Dideberg, O.; Field, M. J. *Proteins* **2003**, *53*, 88−100.
(19) Lamotte-Brasseur, J.; Dive, G.; Dideberg, O.; Charlier, P.; Frere, J. M.; Ghuysen, J. M. *Biochem. J.* **1991**, *279 (Pt 1)*, 213-21.
(20) Diaz, N.; Suarez, D.; Sordo, T. L.; Merz, K. M. *J. Phys. Chem. B* **2001**, *105*, 11302−11313.
(21) Pitarch, J.; Pascual-Ahuir, J. L.; Silla, E.; Tunon, I.; Moliner, V. *J. Chem. Soc., Perkin Trans. 2* **1999**, 1351−1356.
(22) Hermann, J. C.; Ridder, L.; Mulholland, A. J.; Holtje, H. D. *J. Am. Chem. Soc.* **2003**, *125*, 9590−9591.
(23) Pitarch, J.; Pascual-Ahuir, J. L.; Silla, E.; Tunon, I. *J. Chem. Soc., Perkin Trans. 2* **2000**, *4*, 761−767.
(24) Hermann, J. C.; Hensen, C.; Ridder, L.; Mulholland, A. J.; Holtje, H. D. *J. Am. Chem. Soc.* **2005**, *127*, 4454−4465.
(25) Vreven, T.; Morokuma, K.; Farkas, O.; Schlegel, H. B.; Frisch, M. J. *J. Comput. Chem.* **2003**, *24*, 760−769.
(26) Meroueh, S. O.; Roblin, P.; Golemi, D.; Maveyraud, L.; Vakulenko, S. B.; Zhang, Y.; Samama, J. P.; Mobashery, S. *J. Am. Chem. Soc.* **2002**, *124*, 9422−30.
(27) Case, D. A. et al. *AMBER 7*; University of California: San Francisco, 2002.
(28) Bayly, C. I.; Cieplak, P.; Cornell, W. D.; Kollman, P. A. *J. Chem. Phys.* **1993**, *97*, 10269−10280.

was immersed in a box of TIP3P waters,[29] giving an approximately 40 000 atom system. Equilibration involved an energy minimization of 10 000 steps, followed by a 40 ps molecular dynamics simulation while holding the protein and substrate fixed. This was followed by a series of energy minimizations (28 000 steps total) involving gradual decrease of the restraint on the complex from 500 kcal Å^{-2} to 0 kcal Å^{-2}. The system was gradually warmed to 300 K over 48 ps at a constant pressure of 1 atm. Production runs were carried out at constant temperature (300 K) and pressure (1 atm). Coordinates were collected every 0.2 ps. All bonds involving hydrogen atoms were constrained using the SHAKE algorithm with a 2 fs time step.[30] PME electrostatics with periodic boundary conditions were used for all molecular dynamics simulations.[31] Five separate trajectories (about 2 ns each) were carried out for the Michaelis complex, starting with snapshots collected from the first nanosecond of simulation, and giving 10 ns of dynamics. An additional two 1-ns molecular dynamics simulations were carried out for the tetrahedral species and for the acyl-enzyme species with protonated Glu166 and unprotonated Lys73, respectively. The ONIOM method divides the enzyme system into high- and low-level layers connected at the interface by linker atoms. A snapshot from the molecular dynamics simulation provided initial coordinates for the ONIOM QM/MM calculations and was subjected to 50 000 steps of conjugate gradient energy minimization. All water molecules within 20 Å of the penicillanate substrate (295 waters total) were kept for the QM/MM calculations and were included in the MM region (with the exception of the catalytic water molecule, which was included in the QM region). No cutoffs were used during the optimization, and a total of 491 atoms were considered during the optimization. Three partitioning schemes for the QM layer were used for the ONIOM QM/MM calculations. These consisted of optimization at the HF/3-21G level of theory and basis set, followed by a single-point energy calculation using MP2/6-31+G*. This combination has been successfully used in serine proteases with good agreement with experiment.[32] In the first scheme (**QM**$_1$) the QM region consists of the side chains of Glu166, Lys73, and Ser70; the entire β-lactam substrate (penicillanate); and the active-site water. In the second scheme (**QM**$_2$) the QM region consists of the atoms in **QM**$_1$ with the addition of the backbone atoms of Ser70 and Ala237 (comprising the oxyanion hole). In the third scheme (**QM**$_3$), used for probing the β-lactam nitrogen protonation mechanism, the QM region consisted of the atoms in **QM**$_1$ and side chain atoms from Ser130 and Lys234. The same QM region was used for the optimization and energy calculation at the MP2/6-31+G* level. The MM region was treated with the AMBER force field, allowing residues with atoms within 12 Å of the substrate to move during geometry optimization while the rest were held fixed. A total of 346 MP2/6-31+G* calculations (based on 246 HF/3-21G geometry optimizations) were carried out. Potential energy surfaces and potential energy profiles were constructed by incrementing the reaction coordinates by a fixed value, followed by a geometry optimization at the HF/3-21G and single-point energy calculation using MP2/6-31+G* (unless stated otherwise in the text), with the reaction coordinates held fixed.

Results

Penicillanate−TEM β-Lactamase Substrate−Enzyme Pair. The array of functionality at the class A β-lactamase active site is best understood as positioned for general base-catalyzed acylation of the serine and general base-catalyzed transfer of the acyl segment from serine to water. Our computational evaluation of the acylation mechanism uses penicillanic acid as the β-lactamase substrate. Penicillanic acid is a TEM-1 β-lactamase substrate with k_{cat} = 38 s^{-1}, K_m = 295 μM, k_{cat}/K_m = 1.3 × 10^5 M^{-1} s^{-1} (compare to benzylpenicillin k_{cat} = 1200 s^{-1}, K_m = 22 μM, k_{cat}/K_m = 5.5 × 10^7 M^{-1} s^{-1}).[33] Penicillanic acid is a point of reference for comparative β-lactamase computational studies.[18,23,34]

The objective of all computational studies is to discern a more detailed mechanism, especially as relating to the active site machinery involved in proton transfer and bond formation and loss, than that possible from experimental study. In this regard penicillanic acid is an apt choice. Using 6,6-dideuterio-substituted penicillinic acid, Pratt et al. evaluated the β-secondary ^{2}H kinetic isotope effect for penicillanic acid hydrolysis catalyzed by the TEM-2 β-lactamase (for which the penicillanic acid performance constant k_{cat}/K_m = 1.1 × 10^5 M^{-1} s^{-1} is nearly identical to that for TEM-1 enzyme). An inverse β-secondary isotope effect value of 0.926 on the penicillanic acid *V/K* value was observed.[35] Moreover, this β-secondary KIE value was similar to that observed (0.948) for penicillanic alkaline hydrolysis.[36] These values are best interpreted as loss of α-CH hyperconjugation (coinciding to the orbital rehybridization as a nucleophile adds to the adjacent carbonyl) in the rate-limiting transition states of both events.

For the enzymatic hydrolysis, such a transition state, one with substantial tetrahedral character, occurs twice, at the acylation (serine addition) and deacylation (water addition) steps of turnover. It is probable, but certainly not as yet experimentally proven, that acylation rate limits this substrate. The task of assigning chemical identities within the enzymatic hydrolysis mechanism remains a challenge. For TEM acylation, this challenge is best approached within the framework of the nonenzymatic mechanism of β-lactam solvolysis and bearing in mind that the similar ^{2}H β-secondary isotope effects *may* imply similar rate-limiting transition states. Nonenzymatic β-lactam basic solvolysis by water and alcohol nucleophiles is a two-step process involving general base-catalyzed hydroxide (alkoxide) addition to the β-lactam carbonyl, followed by general acid-catalyzed protonation of the amine of the tetrahedral intermediate driving collapse to the ring-opened β-aminocarboxylate product.[37] The rate-limiting step for solution β-lactam hydrolysis is determined by the basicity of the amine of the tetrahedral intermediate and by the reaction pH. For penicillins (wherein the thiazolidine amine basicity in the tetrahedral transition state is relatively weak), the rate-limiting step is hydroxide (alkoxide) addition to the sterically less hindered α (exo) face of the β-lactam. As formation of this tetrahedral intermediate ensues, the nitrogen lone pair develops syn to the incoming nucleophile, providing the necessary nitrogen basicity for the protonation event in tetrahedral collapse.[37]

Based on these observations the generation of a mechanistic hypothesis for TEM serine acylation is straightforward. The penicillin must occupy the active site so as to position the scissile β-lactam carbonyl within bonding distance of the active site

(29) Jorgensen, W. L.; Chandraseklar, J.; Maduar, J. D.; Impey, R. W.; Klein, M. L. *J. Chem. Phys.* **1983**, *79*, 926−935.
(30) Ryckaert, J. P.; Ciccotti, G.; Berendsen, J. H. C. *J. Comput. Chem.* **1977**, *23*, 327−331.
(31) Darden, T. A.; York, D. M.; Pedersen, L. G. *J. Chem. Phys.* **1993**, *98*, 10089.
(32) Zhang, Y. K.; Kua, J.; McCammon, J. A. *J. Am. Chem. Soc.* **2002**, *124*, 10572−10577.
(33) Chaibi, E. B.; Farzaneh, S.; Peduzzi, J.; Barthelemy, M.; Labia, R. *FEMS Microbiol. Lett.* **1996**, *143*, 121−125.
(34) Castillo, R.; Silla, E.; Tunon, I. *J. Am. Chem. Soc.* **2002**, *124*, 1809−16.
(35) Adediran, S. A.; Deraniyagala, S. A.; Xu, Y.; Pratt, R. F. *Biochemistry* **1996**, *35*, 3604−3613.
(36) Deraniyagala, S. A.; Adediran, S. A.; Pratt, R. F. *J. Org. Chem.* **1995**, *60*, 1619−1625.
(37) Page, M. I.; Laws, A. P. In The mechanism of catalysis and the inhibition of β-lactamases. *Chem. Commun.* **1998**, 1611−1617.

Table 1. Average Distances Collected from the Molecular Dynamics Simulations of the Michaelis Complex and the Tetrahedral Species

interaction		distance (Å)								
		Michaelis complex species **I**			tetrahedral species species **III**			acyl-enzyme species **V**		
atom 1	atom 2	R_{min}	R_{max}	$\langle R \rangle$	R_{min}	R_{max}	$\langle R \rangle$	R_{min}	R_{max}	$\langle R \rangle$
Lys73 Nζ	Glu166 Oϵ_1	2.5	3.7	2.9	2.9	5.4	4.2	2.7	5.0	3.6
Lys73 Nζ	Ser130 Oγ	4.3	6.7	5.6	2.5	5.1	3.1	2.6	6.4	4.5
Ser130 Oγ	Ligand O	2.4	4.1	2.7	2.4	3.8	2.8	4.6	9.0	6.3
Ser130 Oγ	Ligand N	3.1	5.0	4.0	2.6	4.1	3.2	4.6	7.3	5.7
Ser130 Oγ	Lys234 Nζ	2.6	5.7	3.3	2.5	4.5	3.4	2.6	7.0	3.7
Ser70 Oγ	Lys73 Nζ	2.5	3.8	3.0	2.5	3.3	2.8	2.7	5.8	4.3
Lys234 Nζ	Ligand O	2.8	6.6	4.3	2.5	3.8	2.7	5.1	11.5	7.9

serine. An amino acid, or ensemble of amino acids, acts as a general base catalyst for serine oxyanion formation. As the tetrahedral species forms, the heavy atom motion must bring the nitrogen lone pair proximal to an amino acid (or amino acid ensemble) for protonation. Last, the heavy atom motion of tetrahedral collapse must properly position the acyl-enzyme within bonding distance of the hydrolytic water (with its own general base machinery) to enable catalytic deacylation.

We have undertaken this comprehensive QM/MM study, supported by extensive molecular dynamics simulations, of TEM acyl-enzyme formation to address the subtle, yet mechanistically critical, aspects of this hypothesis. Which amino acids comprise the general base machinery for the serine? Is the calculated energy path consistent with the expectation of rate-limiting tetrahedral formation? Is the proton that is removed from the serine in tetrahedral intermediate formation the same proton as that delivered to the nitrogen? Is the amino acid ensemble for nitrogen protonation the same, or different, as for serine deprotonation? Does the pathway for tetrahedral collapse provide a catalytically competent acyl-enzyme?

Formation of the Ser70 Tetrahedral Species on the Acylation Pathway. Molecular dynamics simulations of the TEM-1 and penicillanate Michaelis complex (10 ns total) provide insight into the likely pathway for general base activation of Ser70. Lys73 forms hydrogen bonds with both Glu166 (2.9 Å) and Ser70 (3.0 Å), but remains distant (5.6 Å) from Ser130 (Table 1). While Glu166 is not in direct contact with Ser70, a water molecule bridges between the two residues consistently over the 10 ns molecular dynamics simulation (see Figure 1A) in accord with previous simulations.[15,16] Since our molecular dynamics simulations use the AMBER force field, which does not permit bond-forming and bond-breaking, ONIOM QM/MM calculations were used to evaluate reaction pathways and the corresponding energy barriers. These calculations commenced from a snapshot collected from the molecular dynamics simulations using the **QM**$_1$ scheme described above. Prior to construction of a potential energy surface, preliminary calculations evaluated the stability of the Ser70 oxyanion. These calculations addressed the possibility of acylation occurring in a stepwise (that is, a specific base-like) manner where water deprotonates Ser70 followed by nucleophilic addition to the β-lactam carbonyl. These calculations systematically lengthened (at 0.1 Å intervals) the O−H bond of the catalytic water oriented toward Glu166 (d_4 of Figure 1A), subjecting each step to a geometry optimization while holding the reaction coordinate fixed, until the proton was bound to Glu166. The result was unexpected: not only does the proton on Ser70 migrate to the catalytic water (as was expected), but Lys73 is deprotonated in this process by proton transfer from the lysine ammonium group to the Ser70 hydroxyl. To confirm this event, geometry optimization was carried out (B3LYP with a 6-31G* basis set) starting with a protonated Lys73 and a Ser70 oxyanion, obtained by deprotonation by Glu166 through the catalytic water molecule. Geometry optimization again showed spontaneous proton migration from Lys73 to Ser70, giving a protonated Glu166, neutral serine, and free-base Lys73 ensemble. The implication of this proton movement is inescapable. The dominant protonation state of Lys73 in the enzyme−substrate complex is different from that of free enzyme. Whether this is a result of an altered pK_a for Glu166, or for Lys73, or for both, is not material. The presence of substrate in the active site shields the ion pair from solvent resulting in paired neutral Lys73 and Glu166 side chains.

A three-dimensional potential energy surface captured the concerted nature of the reaction. A set of 176 MP2/6-31+G* energy calculations were performed using coordinates from 90 geometry optimizations with HF/3-21G (**QM$_1$** and **QM$_2$** were carried out on the same coordinates obtained from geometry optimization), incrementally altering the distances of the reaction pathway at intervals ranging from 0.05 to 0.2 Å. The reaction coordinate shown in Figure 1A is the difference between (1) the OH bond of the catalytic water (d_4) and the distance between Glu166 Oϵ and water hydrogen (d_3) and (2) the distance between Ser70 Oγ and the carbonyl carbon of the substrate. The first set of 86 MP2/6-31+G* energy calculations were carried out on the smaller QM scheme (**QM$_1$**). A second set of 90 MP2/6-31+G* energy calculations were carried out on the larger QM scheme (**QM$_2$**) incorporating the oxyanion hole. The resulting three-dimensional potential energy surface (based on the **QM$_2$** scheme) is shown in Figure 1B. The surface reveals three energy minima, corresponding to the Michaelis complex with an ion pair for Lys73 and Glu166 (**I**), the Michaelis complex with unprotonated Lys73 and protonated Glu166 (**II**), and the tetrahedral species (**III**). It is of interest to note that both the potential energy surfaces using **QM$_1$** and **QM$_2$** result in the same number of energy minima, and at the same locations on the surface, but with different energy barriers between the minima and relative energies between reactants and products. The energy barriers with the oxyanion hole in the scheme (**QM$_2$**) were consistently lower than those obtained when the hole was not included (**QM$_1$**). These energy barriers are discussed below.

The complete potential energy surface reveals *two* pathways for acylation (Figure 1B). The first (Figure 2B) is indicated by the yellow arrows of Figure 1B. This pathway involves Glu166 proton abstraction from the conserved water molecule, which itself abstracts a proton from Ser70, which then

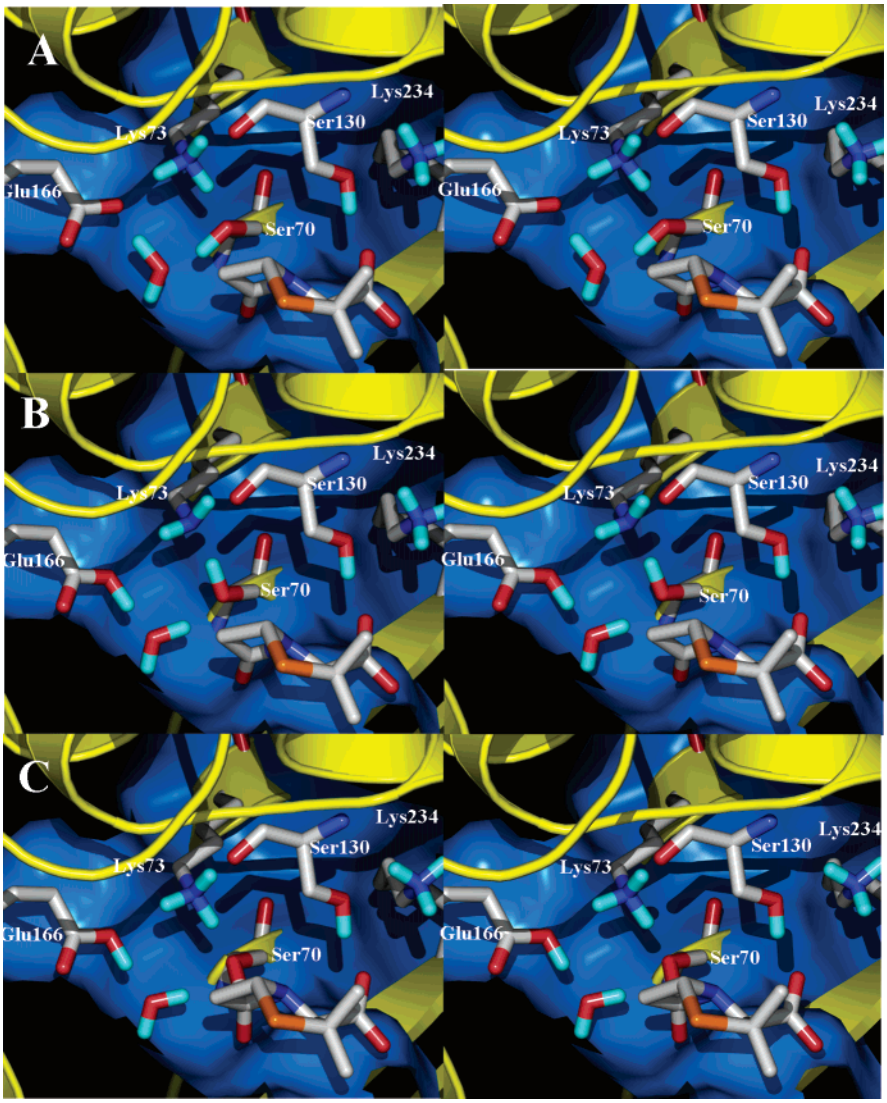

Figure 2. Stereoview representation of (A) species I, (B) species II, and (C) species III, from the potential energy surface in Figure 1B. In each case, residues are shown in capped-sticks representation and atoms are color-coded according to their atom types (S, O, N, C, and H, are shown in orange, red, blue, white, and cyan, respectively). A solvent-accessible surface is constructed around the residues (shown in blue), and the protein is shown in yellow ribbon representation.

removes a proton from Lys73. The energy barrier for this pathway is 10 kcal mol^{-1} using **QM$_1$**, but only 5 kcal mol^{-1} for the larger **QM$_2$**, which includes in the QM layer the protein backbone atoms of the oxyanion hole. The resulting species is either 1 kcal mol^{-1} (**QM$_1$**) or 4 kcal mol^{-1} (**QM$_2$**) lower in energy than the reactant species. The pathway subsequently followed by **II** leading to the formation of the tetrahedral species **III** (Figure 2C) is indicated by the green arrows of Figure 1B. The surface shows this event occurs whereby the free amine of Lys73 abstracts a proton from Ser70. The addition of Ser70 Oγ to the β-lactam carbonyl corresponds to an energy barrier of 22 kcal mol^{-1}. The tetrahedral species **III** is 17 kcal mol^{-1} above **II**.

The second pathway for the formation of the tetrahedral species **III** from **I** is shown by the red arrows of Figure 1B. This pathway is also a concerted event. Glu166 abstraction of a proton from the catalytic water, migration of a proton from Ser70 to the catalytic water, and the bond formation between the Ser70 oxygen and the β-lactam carbonyl occur simultaneously. The computed energy barrier for formation of **III** from **I** is 26 kcal mol^{-1} for **QM$_1$** and 22 kcal mol^{-1} for **QM$_2$**. The energy difference between **I** and **III** is 12 kcal mol^{-1}, indicating that the tetrahedral species is less stable than both reactant states. These results contrast with recent semiempirical QM/MM calculations where the tetrahedral species was found to be more stable than the reactant species by 15 kcal mol^{-1}.[22] Furthermore, the same study reported a potential energy minimum for a hydronium ion during proton transfer from Ser70 to the catalytic water.[22] No such intermediate was found in our study.

The side chain NH bond of Lys73 was not constrained in the geometry optimizations used to construct the potential energy surface shown in Figure 1B. To provide further evidence for the nature of the promotion of Ser70 by Lys73, additional 53 MP2/6-31+G*//HF/3-21G calculations were carried out using **QM$_1$** for the geometry optimization step and **QM$_2$** for the MP2/6-31+G* energy calculation. The resulting surface is shown as Figure 3A. The reaction coordinates are the Lys73 Nζ−H bond (d_7) and the distance between the Ser70 Oγ and the penicillanate carbonyl carbon (d_8). The bonds were incremented at 0.1 Å intervals. The potential energy surface reveals that the conversion of **II** to **III** is concerted and without intermediates (arrows

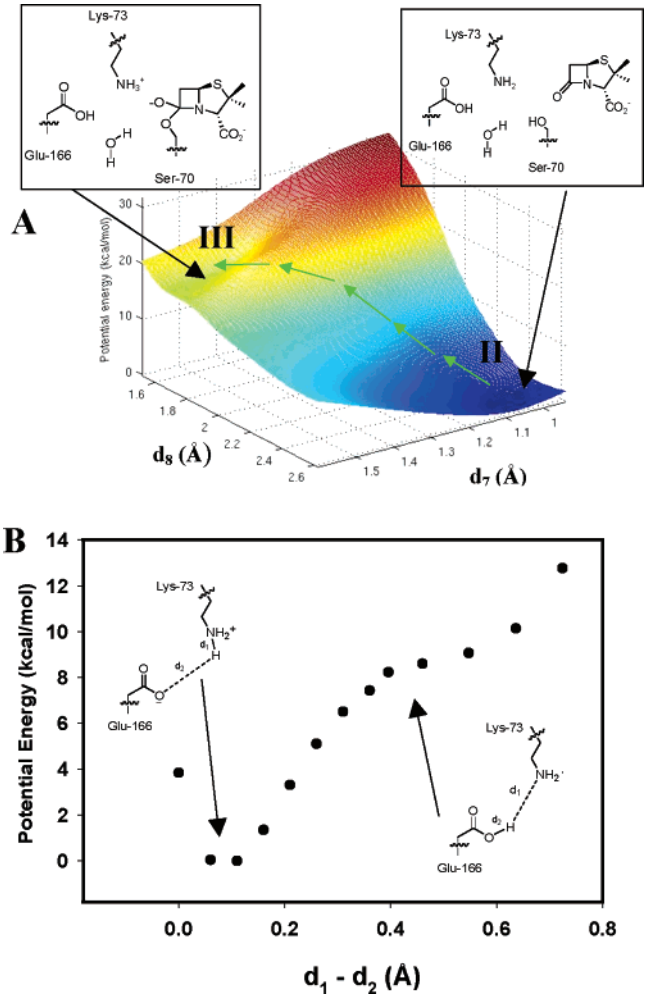

Figure 3. (A) Three-dimensional potential energy surface for the promotion of Ser70 by unprotonated Lys73. (B) Potential energy profile for the direct proton transfer from Lys73 to Glu166.

in Figure 3A). The energy barrier is 22 kcal mol^{-1}. Tetrahedral species **III** is 17 kcal mol^{-1} higher in energy than **II**. These results are consistent with the potential energy surface shown in Figure 1B, which include the OH bond of the catalytic water in the reaction coordinate.

In light of the proximity of the side chains of Lys73 and Glu166 to each other (as seen in numerous X-ray structures and also in the molecular dynamics simulations of this study as tabulated in Table 1), it is no surprise that direct proton transfer from Lys73 to Glu166 was proposed as a likely event to generate the neutral lysine capable of promoting Ser70 for acylation.[21] This particular proton transfer, whereby the proton migrates directly from Lys73 to Glu166 without the intervention of an amino acid residue or a water molecule, is different, however, than the one we propose. The 10 ns molecular dynamics simulations of the TEM-1/penicillanate Michaelis complex that were carried out in the present study reveal a mean distance between Lys73 Nζ and Glu166 Oϵ_1 of 2.9 Å. This suggests that the direct proton transfer is structurally plausible but does not indicate whether it is energetically favorable. Only quantum mechanics can address this issue. Other QM/MM calculations with a semiempirical method found this process to be possible,[21] but later ab-initio-based QM calculations found it implausible.[15] To provide insight into this process, we used ab initio QM/MM calculations with optimization of the QM layer carried out with HF/3-21G followed by MP2/6-31+G* single-point energy calculations. The chosen reaction coordinate was the Lys73 Nζ−H bond. The potential energy profile shown in Figure 3B is the result of 13 calculations using the **QM$_1$** scheme. The energy rises by about 8 kcal mol^{-1} as the proton transfers from Lys73 Nζ to Glu166 Oϵ_1. However, when the proton is located on Glu166 no energy minimum appears for the species, making this process highly unlikely (implicating ready transfer of the Glu166 proton back to Lys73). It is worth mentioning that while the neutral species resulting from the direct proton transfer is the same as **II**, there are important differences in the hydrogen bond network between the two. In the neutral species resulting from a direct proton transfer event the free-base amine of Lys73 is accepting a hydrogen bond from Glu166, and Glu166 accepts a hydrogen bond from the catalytic water molecule, which accepts a hydrogen bond from Ser70. In **II**, however, the amino group of Lys73 accepts a hydrogen bond from Ser70, and Ser70 accepts a hydrogen bond from the catalytic water molecule, which in turn accepts a hydrogen bond from Glu166. This difference is likely the basis for the stability of species **II** when compared to the neutral species resulting from a direct proton transfer from Lys73 to Glu166.

Tetrahedral Collapse to the Acyl-Enzyme. Following tetrahedral formation, nitrogen protonation must occur for scission of the β-lactam C−N bond ring to give the acyl-enzyme. While the closest proton source for this event is the Ser130 hydroxyl, it is not known whether Lys234 or Lys73 acts as the proton source. The involvement of Ser130 in this proton transfer was suggested previously.[13,38] In the Michaelis complex Lys234 is proximal to Ser130, with a mean distance between Ser130 Oγ and Lys234 Nζ of 3.3 Å as compared to the Ser130 Oγ and Lys73 Nζ distance of 5.6 Å. At first glance it is tempting to assume that Lys234 replenishes the proton lost to Ser130. A 1 ns molecular dynamics simulation, starting with **III** (Figure 2C), shed light on this process. The resulting mean distances are listed in Table 1. The results show differences in the configuration of the tetrahedral species when compared to the Michaelis complex. Within the tetrahedral species Lys73 rapidly undergoes a small conformational change, distancing itself from Glu166 and moving toward Ser130. This change results in a mean Ser130 Oγ and Lys73 Nζ separation of 3.1 Å, shorter than the Ser130 Oγ and Lys234 Nζ separation of 3.4 Å. This distance contrasts sharply with the mean separation between Ser130 Oγ and Lys73 Nζ of 5.6 Å seen in the Michaelis complex simulation. Another notable event observed from the simulation is that the Ser130 Oγ no longer forms an exclusive hydrogen bond with the penicillanate carboxylate. It moves instead within hydrogen bonding distance of the β-lactam nitrogen (mean distance of 3.2 Å, as opposed to 4.0 Å in the Michaelis complex). These results show that upon tetrahedral formation a rearrangement occurs wherein Lys73 and Ser130 realign to position for the proton transfer (donated by the Lys73 ammonium) from Ser130 to the nitrogen of **III**, resulting in species **IV** shown in Figure 4A. Acyl-enzyme formation follows. The final event of the acylation pathway is conformational movement of Lys73 closer to Glu166 to enable proton transfer from Glu166 to Lys73 (Figure 4B), poising the Glu166

(38) Wladkowski, B. D.; Chenoweth, S. A.; Sanders, J. N.; Krauss, M.; Stevens, W. J. *J. Am. Chem. Soc.* **1997**, *119*, 6423−6431.

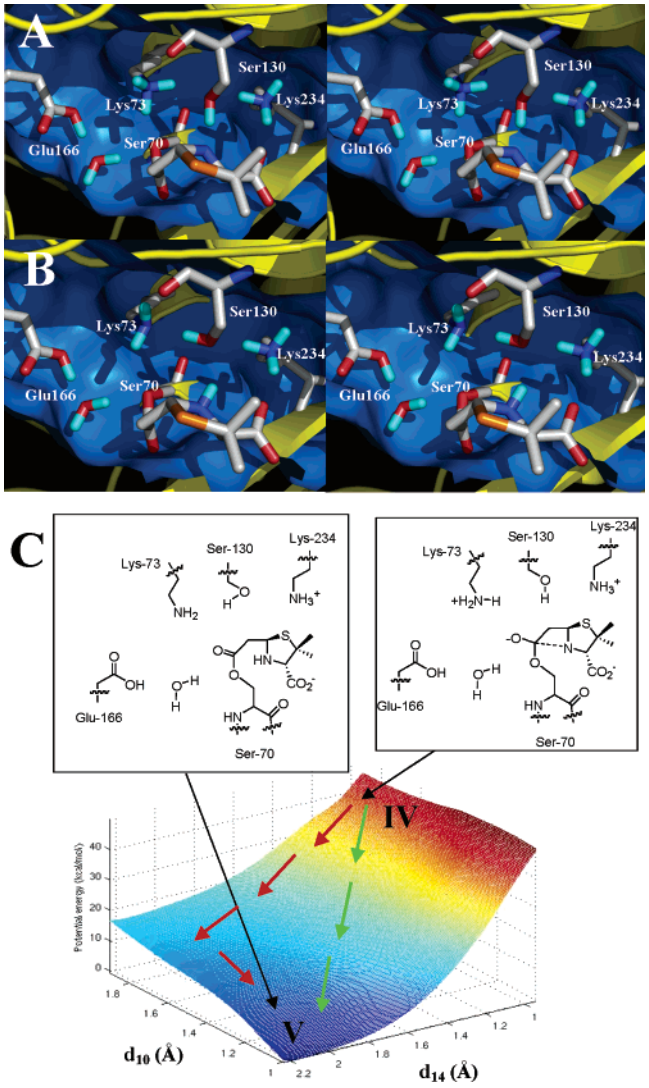

Figure 4. (A) and (B) correspond to a stereoview of species **IV** and **V**, respectively. In each case, residues are shown in capped-sticks representation and atoms are color-coded according to their atom types (S, O, N, C, and H, are shown in orange, red, blue, white, and cyan, respectively). A solvent-accessible surface is constructed around the residues (shown in blue), and the protein is shown in yellow ribbon representation. (C) Three-dimensional potential energy surface for the protonation of the thiazolidine ring following the formation of the tetrahedral species.

carboxylate necessary to initiate deacylation. This proton transfer may occur by the pathway shown in Figure 3B (reverse process).

While the molecular dynamics simulations provide powerful evidence for the role of Lys73 as the proton source for protonation of the β-lactam nitrogen, quantum mechanics would have to be used to describe the proton-transfer event, which involves bond breaking and bond forming events. Starting with a snapshot from the molecular dynamics simulation, a potential energy surface based on 41 QM/MM calculations (optimization of the QM layer carried out with HF/3-21G followed by MP2/6-31+G* single-point energy calculations for each point) was constructed using the **QM$_3$** scheme for the process of protonation of the nitrogen of **IV**. This energy surface is shown in Figure 4C, using as reaction coordinates the Ser130 Oγ and Ser130 Hγ bond (d_9) and the distance between Ser130 Oγ and the Lys73 Nζ (d_{14}). The surface shows no energy minimum for species **IV** (Figure 4B), which forms following the Lys73 movement documented by the molecular dynamics simulation. *It thus appears that once protonated Lys73 approaches Ser130, it readily undergoes deprotonation concomitant with proton migration from Ser130 to the thiazolidine nitrogen, resulting in species **V** shown in Figure 4C.* The process is concerted: proton transfer from Lys73 to Ser130 and from Ser130 to the β-lactam thiazolidine nitrogen occur concomitantly. The stepwise pathway (red arrows in Figure 4), where the proton on Ser130 first transfers to the thiazolidine nitrogen, gives a lower energy species but without a potential energy minimum. Thus, this species also readily converts to **V**. It is of interest to note that during this stepwise pathway, despite the formation of a Ser130 oxyanion, the proton on Lys234 does not migrate to Ser130. This contrasts to the events leading to the tetrahedral species, where deprotonation of Ser70 by Glu166 through the catalytic water immediately leads to the deprotonation of Lys73 to result in a neutral species (**II**). These calculations provide further evidence for a larger Lys234 pK_a compared to Lys73, as the formation of a proximal oxyanion induced proton loss from the latter but not from the former. Furthermore, these calculations substantiate the molecular dynamics conclusion that Lys73, and not Lys234, is the proton source for Ser130 proton transfer to the thiazolidine nitrogen of **III**.

While acyl-enzyme (**V**) results from the protonation event by Ser130 initiating tetrahedral collapse, one final proton migration (from protonated Glu166 to unprotonated Lys73) must occur to complete the acylation half-reaction. But in the species following formation of **V**, Lys73 is engaged in a hydrogen bond with Ser130 (2.8 Å) and is distant from Glu166 (4.2 Å). We resorted to a 1 ns molecular dynamics starting with **V** to shed light on the pathway leading to a conformation where this proton transfer becomes possible. Mean values of the important distances from this simulation are listed in Table 1. These data reveal a reversal of the distances observed for the tetrahedral species: Lys73 is now proximal to Glu166 (3.6 Å) as opposed to Ser130 (4.5 Å). Over the course of the trajectory, Lys73 Nζ approaches Glu166 Oϵ_1 within 3 Å more than 200 times; it is expected that these complexes would readily lead to the proton transfer from Glu166 to Lys73 through a barrierless process, as documented by the potential energy profile shown in Figure 3B. This proton transfer completes the acylation half-reaction and results in the acyl-enzyme complex, which is poised for the Glu166 deacylation event.

A comparison of the potential energy surfaces for the key partial reactions (of **II** to **III** and **IV** to **V**) indicates tetrahedral formation to be the highest energy event, and its computed activation barrier of 22 kcal mol^{-1} is similar to the experimental barrier for TEM-catalyzed penicillanic acid hydrolysis of approximately 16−17 kcal mol^{-1}. We calculate this value from the k_{cat}/K_m ratio for penicillanic acid compared to benzylpenicillin, relative to the estimated activation energy value[24] of 12.7 to 13.7 kcal mol^{-1} for TEM benzylpenicillin hydrolysis. The activation energy for **III** to **IV** is anticipated to be inconsequentially small, and the collapse of tetrahedral intermediate **IV** to the acyl enzyme is very substantially exothermic (by approximately 40 kcal mol^{-1}). By inference the acyl-enzyme is approximately 20 kcal mol^{-1} more stable than the (neutral Lys73) Michaelis complex.

Protonation as the Initiating Event of Tetrahedral Formation. A recent study suggested that β-lactam nitrogen protonation initiates tetrahedral formation, with Ser130 acting as the proton

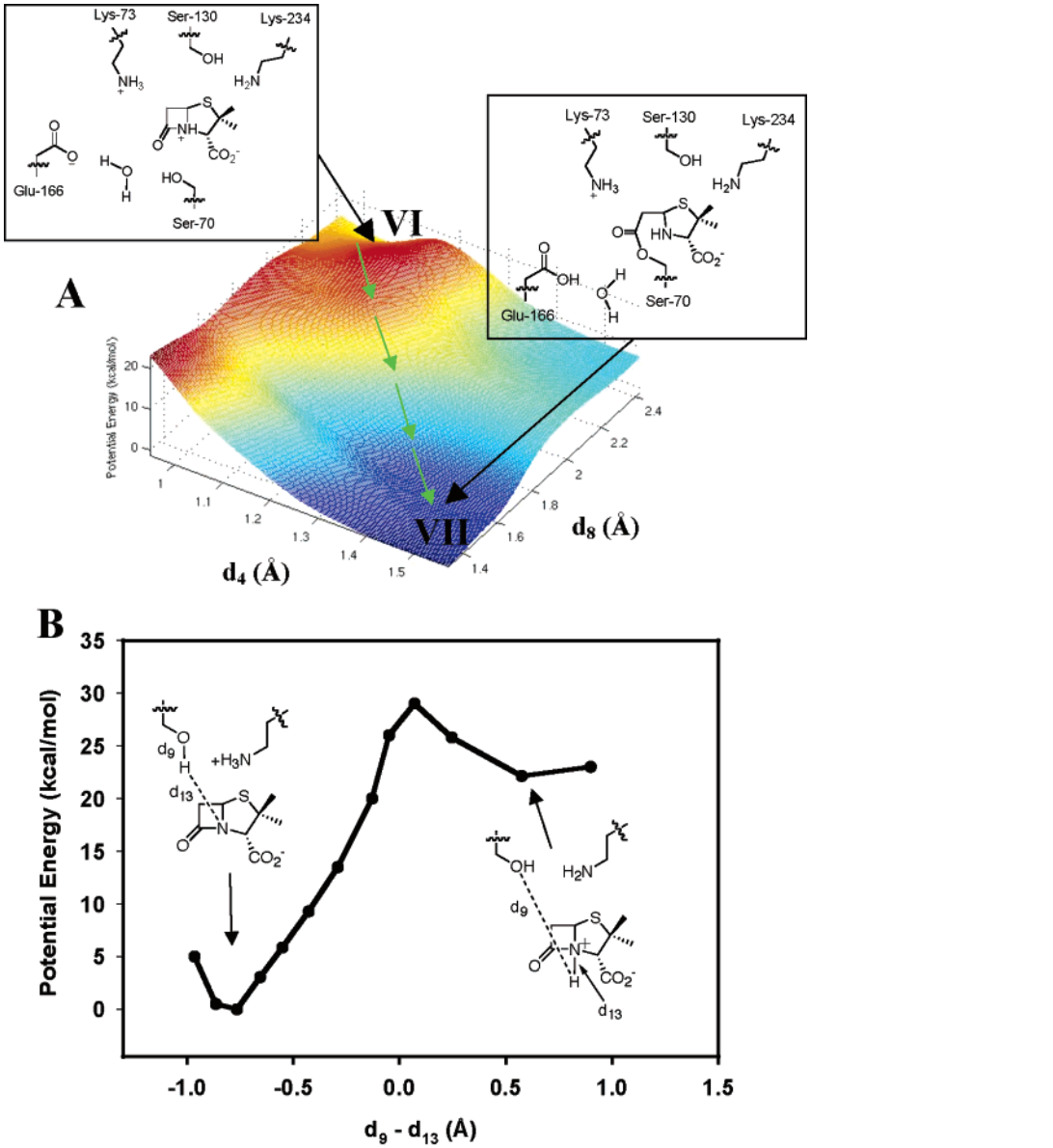

Figure 5. (A) Three-dimensional potential energy surface for the formation of the acyl-enzyme intermediate as a result of protonation of the β-lactam nitrogen. (B) Potential energy profile for the protonation of the β-lactam nitrogen.

donor and Lys234 as the proton source.[17] β-Lactam nitrogen protonation will weaken the C−N bond and reduce the barrier for Ser70 addition to the β-lactam carbonyl. An evaluation of this mechanism was made by construction of a QM/MM three-dimensional potential energy surface for the β-lactam nitrogen protonated intermediate. The first reaction coordinate is the O−H bond of the catalytic water molecule (that points toward Glu166), and the second is the distance between Ser70 Oγ and the β-lactam carbonyl carbon. These reaction coordinates were incremented at 0.1 Å intervals. The resulting surface (based on 40 MP2/6-31+G* calculations using **QM$_2$**) is shown in Figure 5A. The energy barrier for the formation of acyl-enzyme (**VII**) from the protonated β-lactam nitrogen Michaelis complex (**VI**) is 12 kcal mol^{-1}. This calculated barrier is much lower (10 kcal mol^{-1}) than the barriers for the formation of tetrahedral intermediate **III** from species **I** and **II**. Furthermore, the energy of the acyl-enzyme intermediate is 10 kcal mol^{-1} lower than the reactant species **VI**, adding to the favorability of this process. The surface does not show other intermediates.

Yet while serine acylation is highly favorable upon β-lactam nitrogen protonation, one wonders whether this protonation event, equivalent to general *acid* catalyzed acylation, is reasonable. Intuitively, the largest barrier in this mechanism is not tetrahedral formation but the delivery of the proton to the very weakly basic amide of the β-lactam. The 10 ns molecular dynamics simulation shows the Ser130 hydroxyl preferentially hydrogen-bonded to the penicillanic carboxylate in the preacylation species (average 2.7 Å from Ser130 Oγ) rather than to the β-lactam nitrogen (average of 4.0 Å). This makes unlikely donation of a proton by Ser130 to the β-lactam ring. Regardless, should Ser130 act as a proton donor to the ring nitrogen, the molecular dynamics simulations suggest that Lys234 (whose Nζ is 2.6 Å from the Ser130 Oγ) is the more likely proton source to replenish the proton lost by Ser130 (as proposed earlier).[17] Lys73, which is thought to be the proton source following the formation of the tetrahedral species, is unlikely to play that role in the Michaelis complex as the Lys73 Nζ is on average 5.6 Å away from Ser130 Oγ.

The potential energy profile for this proton transfer is shown (Figure 5B). The QM/MM geometry optimizations and energy calculations (based on 13 ONIOM QM/MM MP2/6-31+G* calculations) were carried out with **QM$_3$**. The first reaction coordinate is the Ser130 Oγ−H bond (d_9), and the second is the distance between the β-lactam nitrogen and the Ser130 Hγ (d_{13}). The energy profile reveals a significant increase in energy, a barrier of 29 kcal mol^{-1}, as the proton moves from Ser130 to the β-lactam nitrogen. Moreover, the energy of the resulting species is 22 kcal mol^{-1} higher than the reactants. The barrier for this event exceeds, by 7 kcal mol^{-1}, the barrier for the general base formation of the tetrahedral species. Hence, this mechanism is the least energetically favorable among the three evaluated in this work. The bottleneck to the acyl-enzyme intermediate is indeed the protonation event itself, rather than the ensuing step (which is favorable). It is also of interest to note that these calculations show Lys234, and not Lys73, replenishing the proton lost by Ser130 to the β-lactam nitrogen. This contrasts with the two general base mechanisms where the proton donor is Lys73.

Discussion

The class A β-lactamase mechanism has been subjected to considerable analysis and debate. This is due in large part to the clinical importance of these enzymes, but also as well to puzzling observations from mutant enzyme kinetics. Our preamble to the results concluded with a series of pointed mechanistic questions yet without experimental answers. We have for the catalyst, the TEM β-lactamase, superb crystal structures of its active site, and we have for the substrate of this study, penicillanic acid, a measure of its transition state during catalysis. Meaningful mechanistic reconciliation between structure and transition state is the realm of computation, and we demonstrate here the power of ab initio QM/MM to accomplish this task.

The class A β-lactamase mechanism proceeds via a two-step acylation−deacylation sequence. There is consensus that the deacylation mechanism involves Glu166 general base activation of water addition to the acyl-enzyme. In contrast, the acylation mechanism is contentious. The presumption that acylation also involves general base activation is both reasonable and sensible. The dilemma is the complex array of functionality, a sequestered water, a glutamate carboxylate, a pair of serine hydroxyls (one of which directly participates in the acyl-enzyme), and a lysine, implicated as participants in catalysis by their proximity to the β-lactam. It has been argued that Glu166, via the sequestered water, activates the Ser70 hydroxyl for acylation.[7,17,19,39,40] Others have invoked a free-base Lys73 as the general base.[13,21,23,38,41−43] Not surprisingly, mutations of either Lys73[9,12,39] or Glu166[11,44,45] diminish considerably catalytic ability. The most puzzling mutations are those of Glu166. These mutant enzymes undergo acylation, albeit at attenuated rates. The resulting acyl-enzymes are documented in the X-ray crystal structures of two such mutant enzymes, Glu166Asn and Glu166Ala.[13,14] Here is the quandary. If Glu166 is essential for acylation, why are acylated β-lactamases isolated when it can no longer participate? An argument favoring Glu166 promotion of Ser70 for acylation centers on the premise that the Lys73 pK_a is greater than 10.[40,46,47] Should this lysine have this normal pK_a, its resting state will be as the protonated (and nonbasic) conjugate acid, unable as a general base to promote the serine hydroxyl for acylation. Recent experiments, however, indicate the TEM-1 β-lactamase Lys73 pK_a to be 8.0−8.5.[9] Furthermore, molecular dynamics-based energy calculations using thermodynamic integration argue that when Glu166 is mutated, the pK_a for Lys73 lowers further to approximately 6.0.[9] The attenuation of the lysine pK_a in other enzymes is documented.[48−54] These pK_a alterations are consistent with evolutionary optimization of a general base (or acid) catalyst for maximal efficacy (close alignment of the catalytic functional group pK_a with the operational pH of the enzyme).

β-Lactamases have evolved from parental penicillin-binding proteins.[1,3,8,55−57] Activation of the active site serine in these PBPs occurs by the lysine that corresponds to Lys73 of class A β-lactamases. Loss of Glu166 function (the residue centrally important to deacylation) converts the class A β-lactamase into a "penicillin-binding protein", capable of acylation by β-lactam but incapable of deacylation. The presence of this lysine in the Glu166Ala TEM-1 mutant (albeit with a pK_a = 6.0, and thus a less capable general base)[9] preserves its function as the base in the acylation step. The parental PBP for class A β-lactamases would have a reduced pK_a for the active site lysine, where it serves as the residue that promotes the serine for acylation in the course of catalysis. Introduction of Glu166 in the Ω-loop of class A β-lactamases, a residue critical for the advent of the deacylation step, places the carboxylate of Glu166 proximal to the Lys73 amine. This proximity mandates, for electrostatic reasons, an increase in the pK_a of Lys73 to the experimentally measured value of 8.0−8.5. The consequence of this pK_a (8.0−8.5) is that Lys73 can participate with facility in proton transfer.

Which amino acids, therefore, comprise the general base machinery for the serine? The three proposals for TEM-1 acylation (Glu166 as general base, Lys73 as general base, and a general acid pathway) were investigated by QM/MM analyses. For acylation, these analyses show a concerted Lys73 general

(39) Lietz, E. J.; Truher, H.; Kahn, D.; Hokenson, M. J.; Fink, A. L. *Biochemistry* **2000**, *39*, 4971−81.
(40) Damblon, C.; Raquet, X.; Lian, L. Y.; Lamotte-Brasseur, J.; Fonze, E.; Charlier, P.; Roberts, G. C.; Frere, J. M. *Proc. Natl. Acad. Sci. U.S.A.* **1996**, *93*, 1747−52.
(41) Herzberg, O.; Moult, J. *Science* **1987**, *236*, 694−701.
(42) Swaren, P.; Maveyraud, L.; Guillet, V.; Masson, J. M.; Mourey, L.; Samama, J. P. *Structure* **1995**, *3*, 603−613.
(43) Ishiguro, M.; Imajo, S. *J. Med. Chem.* **1996**, *39*, 2207−2218.
(44) Adachi, H.; Ohta, T.; Matsuzawa, H. *J. Biol. Chem.* **1991**, *266*, 3186−3191.
(45) Escobar, W. A.; Tan, A. K.; Fink, A. L. *Biochemistry* **1991**, *30*, 10783−7.
(46) Lamotte-Brasseur, J.; Lounnas, V.; Raquet, X.; Wade, R. C. *Protein Sci.* **1999**, *8*, 404−409.
(47) Raquet, X.; Lounnas, V.; Lamotte-Brasseur, J.; Frere, J. M.; Wade, R. C. *Biophys. J.* **1997**, *73*, 2416−2426.
(48) Highbarger, L. A.; Gerlt, J. A.; Kenyon, G. L. *Biochemistry* **1996**, *35*, 41−6.
(49) Liu, H. Y.; Zhang, Y. K.; Yang, W. T. *J. Am. Chem. Soc.* **2000**, *122*, 6560−6570.
(50) McKinney, M. K.; Cravatt, B. F. *J. Biol. Chem.* **2003**, *278*, 37393−9.
(51) Highbarger, L. A.; Gerlt, J. A.; Kenyon, G. L. *Biochemistry* **1996**, *35*, 41−46.
(52) Schmidt, D. E., Jr.; Westheimer, F. H. *Biochemistry* **1971**, *10*, 1249−1253.
(53) Daopin, S.; Anderson, D. E.; Baase, W. A.; Dahlquist, F. W.; Matthews, B. W. *Biochemistry* **1991**, *30*, 11521−11529.
(54) Planas, A.; Kirsch, J. F. *Biochemistry* **1991**, *30*, 8268−76.
(55) Moews, P. C.; Knox, J. R.; Dideberg, O.; Charlier, P.; Frere, J. M. *Proteins* **1990**, *7*, 156−171.
(56) Meroueh, S. O.; Minasov, G.; Lee, W.; Shoichet, B. K.; Mobashery, S. *J. Am. Chem. Soc.* **2003**, *125*, 9612−9618.
(57) Kelly, J. A.; Dideberg, O.; Charlier, P.; Wery, J. P.; Libert, M.; Moews, P. C.; Knox, J. R.; Duez, C.; Fraipont, C.; Joris, B.; Dusart, J.; Frere, J. M.; Ghuysen, J. M. *Science* **1986**, *231*, 1429−1431.

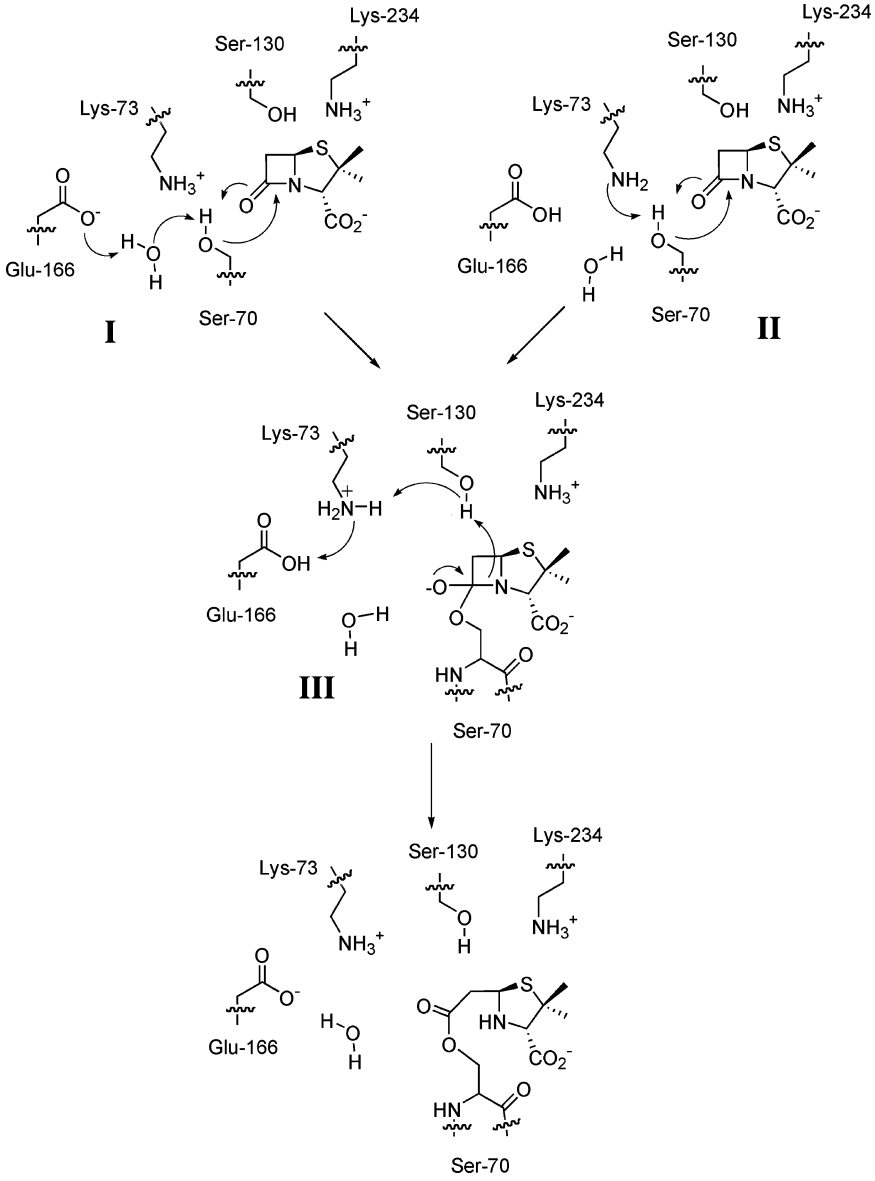

Figure 6. Schematic representing the species that are formed during the acylation half-reaction.

base pathway for the tetrahedral formation, competing favorably with an alternative and only slightly higher in energy (4 kcal mol^{-1}) pathway involving the Glu166 carboxylate as the general base (Figure 6). Lys73 is protonated in the Michaelis complex **I** (Figure 2A). The conversion of **I** to **II** is an exothermic process with a small energy barrier of 5 kcal mol^{-1}, compared to the competing process of the conversion of **I** to **III** which is endothermic and has a barrier of 22 kcal mol^{-1}. Loss of function at Glu166 shuts down the route **I** → **III** (red arrows of Figure 1). This leaves the **II** to **III** route as the only viable acylation pathway (yellow and green arrows of Figure 1). Similarly, mutation of Lys73 to arginine severely impairs, but does not abolish, catalysis.[12] The converse happens in this case: the conversion of **I** → **II** → **III** becomes difficult (if not impossible) leaving the **I** → **III** sequence as the viable recourse to acylation. Not surprisingly, neither mutation at Lys73 nor at Glu166 is seen among the 133 clinical variants of the TEM-1 β-lactamase. Molecular dynamics simulations starting with tetrahedral intermediate **III** show the Lys73 conjugate acid as the proton source, and Ser130 as the immediate proton donor, enabling the proton transfer to the nitrogen of **III** resulting in species **IV**. This protonation drives tetrahedral collapse to acyl-enzyme **V**. The class A β-lactamase active site is the product of finely tuned evolution,[58] where both Lys73 and Glu166 are needed for catalytic competence.

Are the calculated energy paths consistent with the expectation of rate-limiting tetrahedral formation? The rate-limiting step in base solvolysis of β-lactams is hydroxide (alkoxide) tetrahedral formation, and the anticipation that β-lactamases have evolved to stabilize this transition state, which is unique to β-lactams, is unassailable. A degree of transition state stabilization enabling true Brønsted general base catalysis (characterized by concerted proton motion) is demanded by the magnitude of the β-lactamase V/K, and it is enormously gratifying that the potential energy surfaces of Figures 1 and 3 (for both the Glu166 and Lys73 pathways) reflect this expectation. Moreover, we know from Pratt's elegant kinetic study on TEM catalyzed penicillanic acid hydrolysis that the transition state

(58) Hardy, L. W.; Kirsch, J. F. *Biochemistry* **1984**, *23*, 1275−82.

that it experiences is consistent with these potential energy surfaces.

Is the proton that is removed from the serine in tetrahedral intermediate formation the same proton as is delivered to the nitrogen? Is the amino acid ensemble for nitrogen protonation the same, or different, as for serine deprotonation? The answer to the first question (Figures 4 and 5) is emphatic. It is not. And while the answer to the second question is as emphatic, they are, these simple responses beg the question as to why the acylation mechanism of this β-lactamase encompasses such convoluted proton motion. A dual mechanism in tetrahedral formation is understandable in terms of Glu166 acquisition as a means of augmenting catalytic acylation (to an ancestral PBP, where this was already enabled) and empowering catalytic deacylation. It is useful, in considering possible answers as to the purpose behind the complex proton motion of tetrahedral formation and collapse, to remember that evolutionary optimization of enzymatic activity is driven by acquisition of function, not acquisition of simplicity. As Page has emphasized, catalysis of nucleophilic β-lactam opening requires *proximal* juxtaposition of the base (for tetrahedral formation) and acid (for tetrahedral collapse). Yet these cannot coexist (should this happen, they would self-annihilate by proton transfer). The convoluted proton motion of these two steps likely reflects the solution, accomplished by this enzyme, to this conundrum.

Does the reaction pathway for tetrahedral collapse provide a catalytically competent acyl-enzyme? This question must be parsed into two separate questions. Does the heavy-atom motion properly position the acyl-enzyme? The torsional atom motion in tetrahedral collapse is constrained by the oxyanion hole, and the stereoelectronics of the tetrahedral intermediate. The computations show that tetrahedral collapse leads to smooth alignment of the acyl-enzyme adjacent to the hydrolytic water (Figure 4). Second, is the catalytic functional group for deacylation in the protonation state required for the next step of catalysis? While tetrahedral collapse gives the glutamic acid as the free acid (and not the carboxylate that is required for deacylation), the computations also demonstrate ideal Lys73 positioning for facile proton back transfer to activate the glutamate (Figure 3B).

Last, brief comments are presented as to what differentiates our computations from those reported previously. Unlike previous studies, the QM layer was treated with ab initio molecular orbital calculations at the MP2/6-31+G* level. This is superior to semiempirical calculations. Furthermore, solvent water molecules are explicitly included in the MM region of the QM/MM calculations, and the catalytic water is included in the QM region. The QM layer experiences the effects of the atomic charge of these water molecules, and other protein residues, in the MM layer. Last, a comparison to the QM/MM study of TEM acylation by benzylpenicillin reported by Hermann et al. (made using a complementary B3LYP/AM1-CHARMM22 method) shows points of similarity and of difference. The first similarity is the presence of a concerted Glu166 general base mechanism, operating through the water molecule, for promotion of serine addition to the β-lactam. The second is the Ser130 relay for Lys73 ammonium protonation of the thiazolidine nitrogen, enabling tetrahedral intermediate collapse to the acyl-enzyme. In the computation of Hermann et al., proton transfer from Glu166 participates in this relay, whereas we see this as a subsequent event. This divergence is inconsequential (especially when it is further noted that the two computations use different substrates). Two differences separate our computations from those of Hermann et al. The first is our finding of a fully viable Lys73 general base mechanism. Its appearance as a credible pathway in our study is an outcome of the ab initio method, whereas the protonated K73 constraint of the QM set of Hermann et al. precluded its appearance in their study. In the broader perspective, however, this outcome must be understood more as a point of difference than of disagreement. The value of the β-lactamase to the bacterium rests in its ability to hydrolytically detoxicate a remarkably diverse array of β-lactam structure. Depending on the particular structure presented to the active site, one pathway may be used in preference to the other. The second (and more significant) difference between our study and that of Hermann et al. is the relative energy of the tetrahedral intermediate. In their B3LYP/AM1-CHARMM22 computations these intermediates are more stable than the Michaelis complex, whereas in our ab initio determinations these are metastable intermediates, well elevated from the ground state. This must reflect a fundamental difference between the computational methods, and also from the choice of atoms in the QM set. Beyond this facile conclusion we are unable to identify a particular origin of the very different predicted energies by the two methods. We note in passing that elevated energies for serine tetrahedral intermediates in the oxyanion hole have been encountered in other high-level enzyme calculations with serine proteases.[59] Moreover, a relatively high energy content for this tetrahedral intermediate is intuitive. There is no driving evolutionary force for the enzyme to stabilize a transition state—or an intermediate—below the point that the necessary k_{cat}/K_m has been achieved. Rather, it must be anticipated that preserving the energy content of one intermediate, so as to diminish the activation energy for progression to the next intermediate, is advantageous. This is what we observe in our study: the protonation of the initial tetrahedral intermediate results in the spontantaneous and energetically favorable collapse to the acyl enzyme.

The steps governing acylation in the class A β-lactamase active site have been visualized. These results explain the seemingly conflicting findings from mutagenesis studies and reconcile a duality for Glu166 and Lys73 in serine activation. Class A β-lactamases represent a case study of how a basic structural template, shared with the bacterial PBP catalysts of cell wall biosynthesis, has undergone adaptation to expand the repertoire of reactions needed by the bacterium.

Acknowledgment. "A photograph of a horse does not necessarily tell you how fast it can run." This paper is dedicated, with personal affection (J.F.F.) and professional admiration, to Jeremy Knowles, on the occasion of his 70th birthday and in tribute to his numerous mechanistic contributions toward the understanding of this enzyme. This research was supported by the National Institutes of Health.

Supporting Information Available: Complete ref 27. This material is available free of charge via the Internet at http://pubs.acs.org.

JA051592U

(59) Ishida, T.; Kato, S. *J. Am. Chem. Soc.* **2003**, *125*, 12035−12048.